

# Selective intercalation of six ligand molecules in a self-assembled triple helix

Miguel A. Mateos-Timoneda, Jessica M. C. A. Kerckhoffs, David N. Reinhoudt\* and Mercedes Crego-Calama\*

Received 7th December 2006, Accepted 11th December 2006

First published as an Advance Article on the web 5th January 2007

DOI: 10.1039/b617895b

The addition of a ligand molecule to an artificial self-assembled triple helix leads to the selective intercalation of two hydrogen-bonded trimers in specific binding pockets. Furthermore, the triple helix suffers large conformational rearrangements in order to accommodate the ligand molecules in a highly organized manner.

## Introduction

Self-assembly is Nature's preferred pathway for the formation of complex structures with biological activity.<sup>1</sup> It denotes the spontaneous connection of a few (or many) components into discrete and well-defined structures.<sup>2</sup> Thus, self-assembly is one of the key approaches for the creation of nanostructures and nanodevices with biological properties.<sup>3</sup> In this research area much attention has been focused on the design of functional synthetic biomolecules such as proteins<sup>4</sup> and DNA mimics.<sup>5</sup> Besides control over the self-assembly of these structures, understanding of the binding of organic ligands to natural biomolecules and the way natural molecules can be mimicked is essential to achieve functionality.<sup>6</sup> For example, numerous publications dealing with the interaction of quadruplex-specific ligands with G-tetrads have been reported.<sup>7</sup> This type of ligand molecules can stabilize the four-stranded quadruplex structure of a single-stranded DNA primer. They are potential inhibitors of the telomerase function, which is important for the replication of cancer cells.<sup>8</sup>

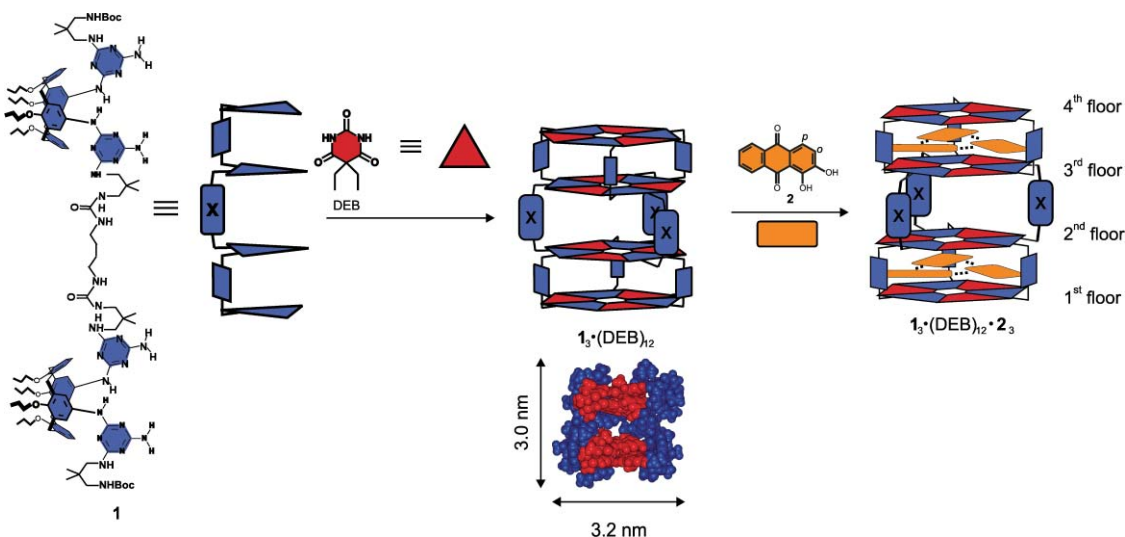
In this paper, we show how the self-assembly of synthetic structures that are structural mimics of DNA complexes can be controlled. We describe the selective and site-specific intercalation of two self-assembled trimeric ligands in distinct solvophobic cores of an artificial triple hydrogen-bonded helix, the so called tetra-rosette assembly.<sup>9</sup>

## Results and discussion

A tetra-rosette consists of 15 components (three tetramelamine strands **1** formed by two calix[4]arene dimelamine units covalently connected through a flexible linker **X** and twelve 5,5-diethylbarbiturates (DEB)) held together by 72 hydrogen bonds forming the triple helix  $\mathbf{1}_3 \cdot (\text{DEB})_{12}$  with four parallel rosette "floors" (Scheme 1). The three orthogonal acceptor–donor–acceptor (ADA) hydrogen bonding arrays of DEB are complementary to the three DAD hydrogen bonding arrays of the melamines. The resulting nanostructure has a height of  $\sim 3.0$  nm and a width of  $\sim 3.2$  nm. The thermodynamic equilibrium for this type of assembly is reached within seconds after mixing the corresponding building blocks.<sup>9</sup>

The first evidence for the complexation of the ligands by the triple helix comes from <sup>1</sup>H NMR spectroscopy. Addition of ligand

Laboratory of Supramolecular Chemistry and Technology, MESA<sup>+</sup> Institute for Nanotechnology, Faculty of Sciences and Technology, University of Twente, P. O. Box 217, 7500AE Enschede, The Netherlands



**Scheme 1** Schematic representation of the building blocks and assembly formation of tetra-rosette  $\mathbf{1}_3 \cdot (\text{DEB})_{12}$ . The molecular structure of the guest molecule **2** and its encapsulation forming complex  $\mathbf{1}_3 \cdot (\text{DEB})_{12} \cdot \mathbf{2}_6$  is also shown. For clarity, in the molecular modeling picture of the assembly one tetramelamine moiety and hydrogen atoms have been omitted.

**2** (6 equivalents) to  $\mathbf{1}_3 \cdot (\text{DEB})_{12}$  showed remarkable shifts in the  $^1\text{H}$  NMR signals of both host and ligand molecules (Fig. 1). For example, the  $\text{NH}_{\text{DEB}}$ -protons (Ha and Hb) showed upfield shifts from 14.17, 13.73, 13.33, and 12.96 ppm to 13.11, 12.93, 12.84, and 12.66 ppm (Fig. 1). Furthermore, the majority of the signals of the ligand molecules are shifted upfield by  $\geq 3$  ppm indicating the encapsulation of **2**. The integration of the  $^1\text{H}$  NMR signals yielded a 6 : 1 ratio for the complexation of **2** by  $\mathbf{1}_3 \cdot (\text{DEB})_{12}$ . Furthermore, the  $\text{OH}^n$  of **2** is shifted downfield, indicating the formation of an intermolecular hydrogen bond between this proton and the carboxyl group of the adjacent guest molecule.<sup>10</sup> Careful inspection of the  $^1\text{H}$  NMR spectrum shows that two trimers of **2** are encapsulated by the tetra-rosette  $\mathbf{1}_3 \cdot (\text{DEB})_{12}$ , one in between the 1<sup>st</sup> and the 2<sup>nd</sup> floors and one in between 3<sup>rd</sup> and the 4<sup>th</sup> rosette floors. The encapsulation in each pocket is similar to the encapsulation of alizarin by double rosette assemblies,<sup>10</sup> thus showing highly specific intercalation between the layers of each individual double rosette and not in the cavity formed between the two double rosette motifs, as shown for other guest molecules.<sup>11</sup>

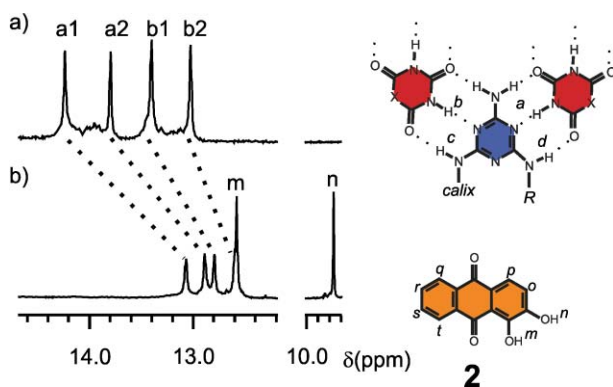


**Fig. 1** Parts of the  $^1\text{H}$  NMR spectra (300 MHz) of (a) tetra-rosette assembly  $\mathbf{1}_3 \cdot (\text{DEB})_{12}$ , (b) after the addition of 6 eq. of alizarin **2**. Spectra in  $\text{CDCl}_3$  at 293 K. (NHa1-b1, first and fourth floors and NHa2-b2, second and third floors of the tetra-rosette assembly  $\mathbf{1}_3 \cdot (\text{DEB})_{12}$ , Scheme 1).

For complex  $\mathbf{1}_3 \cdot (\text{DEB})_{12} \cdot \mathbf{2}_6$ , in the  $^1\text{H}$  NMR spectrum four signals were observed in the region between 13–15 ppm (Fig. 1b), indicating that assembly  $\mathbf{1}_3 \cdot (\text{DEB})_{12}$  can only exist as the *SSS*-, *SES*-, or *EEE*-isomer (*S* = staggered, *E* = eclipsed).<sup>12</sup> Earlier results have demonstrated that assembly  $\mathbf{1}_3 \cdot (\text{DEB})_{12}$  exists only as the *SSS*-isomer.<sup>9</sup> Thus, encapsulation of two **2**<sub>3</sub> by the tetra-rosette assembly *SSS*- $\mathbf{1}_3 \cdot (\text{DEB})_{12}$  would give 4 or 8 signals in the  $^1\text{H}$  NMR spectrum for the  $\text{NH}_{\text{DEB}}$ -protons, depending on whether the two **2**<sub>3</sub> trimers are encapsulated with the same or different orientation, respectively (Fig. 2).<sup>10</sup> However, if similar behavior to double rosettes<sup>10</sup> is expected, the encapsulation of **2** by tetra-rosette assembly  $\mathbf{1}_3 \cdot (\text{DEB})_{12}$  should change the relative orientation of the rosette floors from staggered to symmetrical eclipsed. Conformational isomers *ESE* and *EEE* show a symmetrical eclipsed conformation for the two double rosettes of assembly  $\mathbf{1}_3 \cdot (\text{DEB})_{12}$ . Based on the number of signals observed in the  $^1\text{H}$  NMR spectrum the *EEE*-isomer is the most likely to be formed.<sup>13</sup>

Additionally, gas-phase molecular minimization studies of the complex show the formation of the isomer with *EEE* orientation (Fig. 3).

A  $^1\text{H}$  NMR titration experiment of the encapsulation of **2** (up to approximately 6 equivalents<sup>14</sup>) by  $\mathbf{1}_3 \cdot (\text{DEB})_{12}$  (1.0 mM

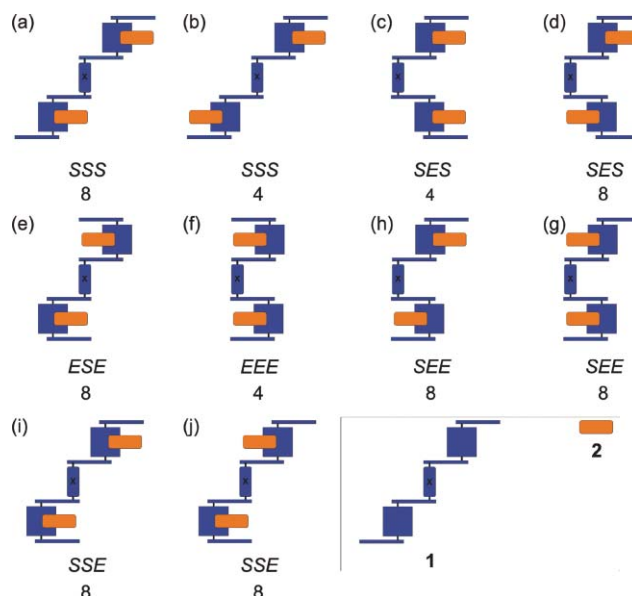


**Fig. 2** Schematic representation of all possible isomers of a tetra-rosette assembly. (Blue squares are calix[4]arenes and orange rectangles are alizarins). Only assemblies with  $C_3$ -axes are considered, which means that all 3 tetramelamines have the same orientation. The isomers are coded with 3 letters (*S* for staggered and *E* for eclipsed). The number of signals expected in the  $^1\text{H}$  NMR spectrum (15–12 ppm) for the different isomers are given below the schematic representation.

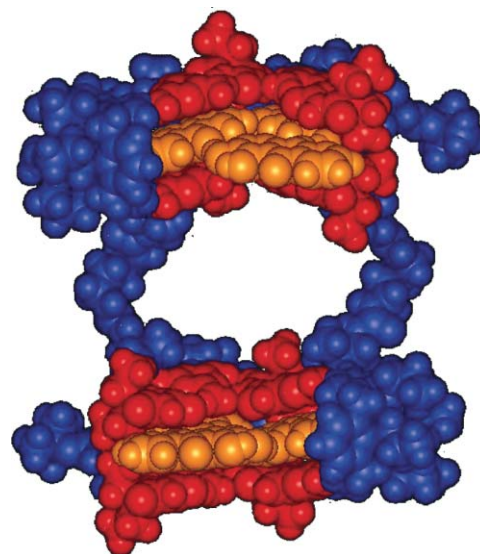


**Fig. 3** Gas-phase minimized structure of the *EEE*-isomer of  $\mathbf{1}_3 \cdot (\text{DEB})_{12} \cdot \mathbf{2}_6$ . For clarity hydrogen atoms as well as one tetramelamine moiety are omitted.

in  $\text{CDCl}_3$ ) showed two sets of new signals in the 15–12 ppm region after the addition of 3 eq. of **2**, as well as two signals around 9.7–9.5 ppm. One of the sets corresponds to the formation of a complex with only one **2**<sub>3</sub> trimer,  $\mathbf{1}_3 \cdot (\text{DEB})_{12} \cdot \mathbf{2}_3$ . Based on the intensities observed for the  $\text{NH}_{\text{DEB}}$ -protons, the ratio of the assemblies  $\mathbf{1}_3 \cdot (\text{DEB})_{12} : \mathbf{1}_3 \cdot (\text{DEB})_{12} \cdot \mathbf{2}_3 : \mathbf{1}_3 \cdot (\text{DEB})_{12} \cdot \mathbf{2}_6$  is 1 : 1 : 1. These relative concentrations indicated that the formation of each trimer **2**<sub>3</sub> is strongly cooperative, but the complexation of the first **2**<sub>3</sub> trimer does not significantly influence the complexation of

the second  $2_3$  trimer. Moreover, the encapsulation of alizarine is highly selective because similar molecules, such as anthracene and 1,2,5,8-tetrahydroxyanthraquinone are not encapsulated.

## Conclusion

The results described in this article provide an unprecedented example of the encapsulation of ligand molecules in synthetic self-assembled helices resembling the intercalation mode encountered in the guanine-rich region of DNA.<sup>7</sup> Moreover, the encapsulation displays high selectivity and specificity both for the guest molecule and the region of the host assembly. Upon ligand intercalation, large conformational changes in the host structure are also observed.<sup>15</sup> It is also important to outline here that the self-assembly of the receptor and the recognition processes bring together, using the same noncovalent interactions, fifteen building blocks of the receptor and six guest molecules with absolute control over their spatial disposition.

## Experimental

<sup>1</sup>H NMR spectra were recorded on a Varian Unity 300 spectrometer or on a Varian Unity 400 WB spectrometer. Residual solvent protons were used as an internal standard and chemical shifts are given relative to tetramethylsilane (TMS) or to the residual solvent protons. The 2D DQF-COSY consisted of 2048 datapoints in  $t_2$  and 512 increments in  $t_1$ . The data were apodized with a shifted sine-bell square function in both dimensions and processed to a 4 K × 1 K matrix. For the TOCSY experiment, the total TOCSY mixing time was set to 65 ms. The spectrum was acquired with 1024 data points in  $t_2$  and 512 FIDs in  $t_1$ . The data were apodized with a shifted sine-bell square function in both dimensions and processed to a 2 K × 2 K matrix. The NOESY experiments were acquired with a mixing time of 150 ms, 2K datapoints in  $t_2$  and 512 increments in  $t_1$ .

## Synthesis

Tetramelamine **1** was synthesized following methods described previously.<sup>9</sup>

### Formation of assemblies $1_3\cdot(\text{DEB})_{12}$

Hydrogen bonded assembly  $1_3\cdot(\text{DEB})_{12}$  was prepared by mixing calix[4]arene tetramelamine **2** with 4 equivalents of DEB in CDCl<sub>3</sub> for 15 minutes. For example, 7.02 mg (0.003 mmol) of **1** and 2.20 mg (0.012 mmol) of DEB were dissolved in 5 ml of CDCl<sub>3</sub>, and stirred until all the compounds were dissolved. After evaporation of the solvent under high-vacuum, the assembly was ready to use.

### Molecular mechanics calculations

Initial structures, created by manual modification of the X-ray structure of a double rosette assembly,<sup>10,16</sup> and by observed NOE connectivities used as distance constraints, as well as visualizations were carried out with Quanta 97.<sup>17</sup> The MD calculations were run with CHARMM, version 24.0.<sup>18</sup> Parameters were taken from Quanta 97, and point charges were assigned with the charge template option in Quanta/CHARMM; excess charge

was smoothed, rendering overall neutral residues. A distance-dependent dielectric constant was applied with  $\epsilon = 1$ . No cut-offs on the nonbonded interactions were used. Energy-minimizations were performed with the Steepest Descent and Adopted Basis Newton–Raphson methods until the root mean square of the energy gradient was  $<0.001 \text{ kcal mol}^{-1} \text{ \AA}^{-1}$ .

## Acknowledgements

This work is partially supported by the Technology Foundation of The Netherlands (J. M. C. A. K.). The research of M. C.-C. has been made possible by a fellowship of the Royal Netherlands Academy of Arts and Sciences.

## References

- 1 R. Fiammengo, M. Crego-Calama and D. N. Reinhoudt, *Curr. Opin. Chem. Biol.*, 2001, **5**, 660–673.
- 2 G. M. Whitesides and B. Grzybowski, *Science*, 2002, **295**, 2418–2421; J.-M. Lehn, *Supramolecular Chemistry: Concepts and Perspectives*, VCH, Weinheim, 1995.
- 3 S. De Feyter and F. C. De Schryver, *Chem. Soc. Rev.*, 2003, **32**, 139–150; D. Philp and J. F. Stoddart, *Angew. Chem., Int. Ed. Engl.*, 1996, **35**, 1154–1196.
- 4 R. B. Hill, D. P. Raleigh, A. Lombardi and W. F. DeGrado, *Acc. Chem. Res.*, 2000, **33**, 745–754.
- 5 F. Rakotonradany, A. Palmer, V. Toader, B. Chen, M. A. Whitehead and H. F. Sleiman, *Chem. Commun.*, 2005, 5441–5443.
- 6 A. J. Doerr, M. A. Case, I. Pelczera and G. L. McLendon, *J. Am. Chem. Soc.*, 2004, **126**, 4192–4198.
- 7 M. A. Read and S. Neidle, *Biochemistry*, 2000, **39**, 13422–13432; G. R. Clark, P. D. Pytel, C. J. Squire and S. Neidle, *J. Am. Chem. Soc.*, 2003, **125**, 4066–4067.
- 8 E. Gavathiotis, R. A. Heals, M. F. G. Stevens and M. S. Searle, *Angew. Chem., Int. Ed.*, 2001, **40**, 4749–4751.
- 9 K. A. Jolliffe, P. Timmerman and D. N. Reinhoudt, *Angew. Chem., Int. Ed.*, 1999, **38**, 933–937; L. J. Prins, E. E. Neuteboom, V. Paraschiv, M. Crego-Calama, P. Timmerman and D. N. Reinhoudt, *J. Org. Chem.*, 2002, **67**, 4808–4820.
- 10 J. M. C. A. Kerckhoffs, F. W. B. van Leeuwen, A. L. Spek, H. Kooijman, M. Crego-Calama and D. N. Reinhoudt, *Angew. Chem., Int. Ed.*, 2003, **42**, 5717–5722; J. M. C. A. Kerckhoffs, M. G. J. ten Cate, M. A. Mateos-Timoneda, F. W. B. van Leeuwen, B. Snellink-Ruël, A. L. Spek, H. Kooijman, M. Crego-Calama and D. N. Reinhoudt, *J. Am. Chem. Soc.*, 2005, **127**, 12697–12708; M. A. Mateos-Timoneda, J. M. C. A. Kerckhoffs, M. Crego-Calama and D. N. Reinhoudt, *Angew. Chem., Int. Ed.*, 2005, **44**, 3248–3253.
- 11 T. Ishi-i, M. A. Mateos-Timoneda, P. Timmerman, M. Crego-Calama, S. Shinkai and D. N. Reinhoudt, *Angew. Chem., Int. Ed.*, 2003, **42**, 2300–2305.
- 12 The isomers of assembly  $1_3\cdot(\text{DEB})_{12}$  are coded with three letters (*S* for staggered; *E* for eclipsed), which represent the relative orientation of the melamine fragments between the rosette layers 1<sup>st</sup> and 2<sup>nd</sup>, 2<sup>nd</sup> and 3<sup>rd</sup>, and 3<sup>rd</sup> and 4<sup>th</sup> floors, respectively.
- 13 Based on symmetry reasons, isomer *ESE* will give 8 signals in the <sup>1</sup>H NMR spectrum.
- 14 Due to the low solubility of **2**, only a titration up to 6 eq. was carried out.
- 15 S. Bouaziz, A. Keltani and D. J. Patel, *J. Mol. Biol.*, 1998, **282**, 637–652.
- 16 P. Timmerman, R. H. Vreekamp, R. H. Hulst, W. Verboom, D. N. Reinhoudt, K. Rissanen, K. A. Udachin and J. Ripmeester, *Chem.–Eur. J.*, 1997, **3**, 1823–1832.
- 17 Quanta97 *Molecular Simulations*, Waltham, MA, 1997.
- 18 B. R. Brooks, R. E. Bruccoleri, B. D. Olafsen, D. J. States, S. Swaminathan and M. J. Karplus, *J. Comput. Chem.*, 1983, **4**, 187–217; F. A. Momany, V. J. Klimkowski and L. J. Schäfer, *J. Comput. Chem.*, 1990, **11**, 654–662; F. A. Momany, R. Rone, H. Kunz, R. F. Frey, S. Q. Newton and L. J. Schäfer, *J. Mol. Struct.*, 1993, **286**, 1–18.